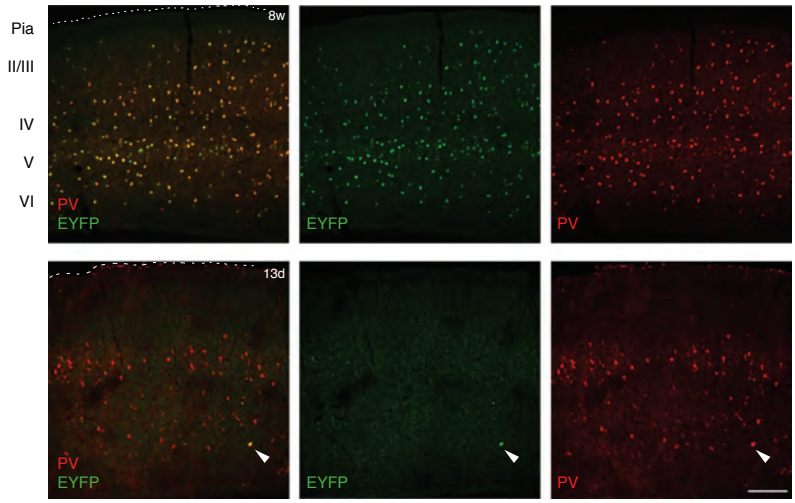

Supplementary Figure 1

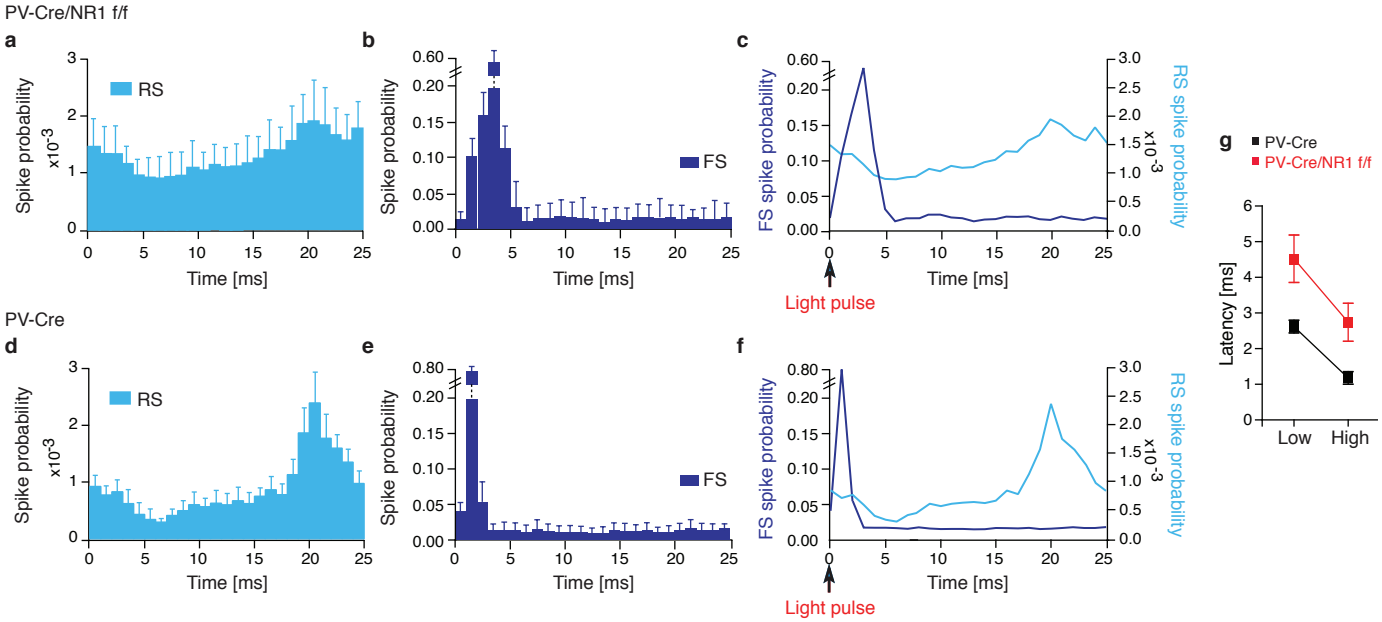

Supplementary Figure 2

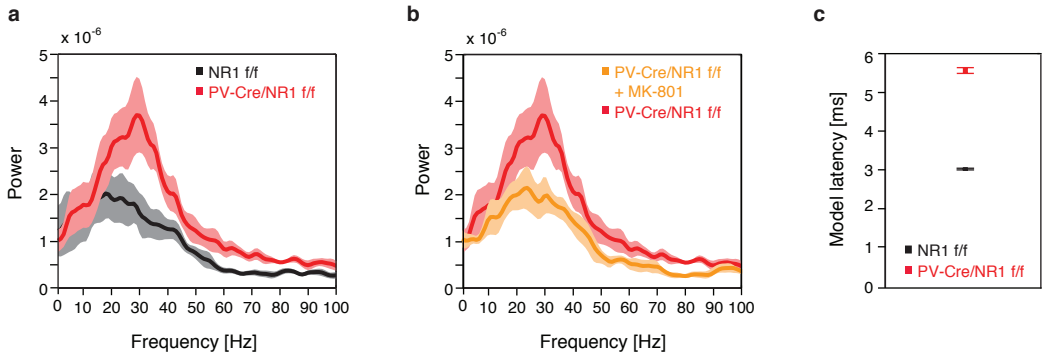

Supplementary Figure 3

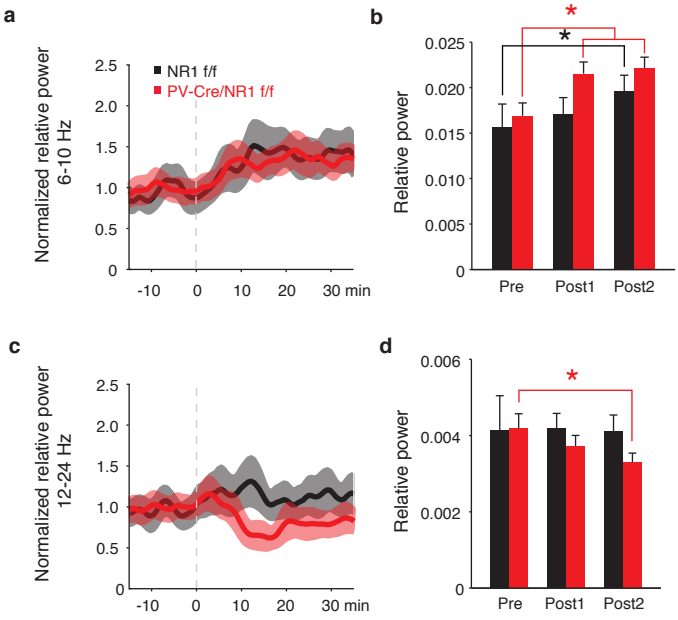

Supplementary Figure 4

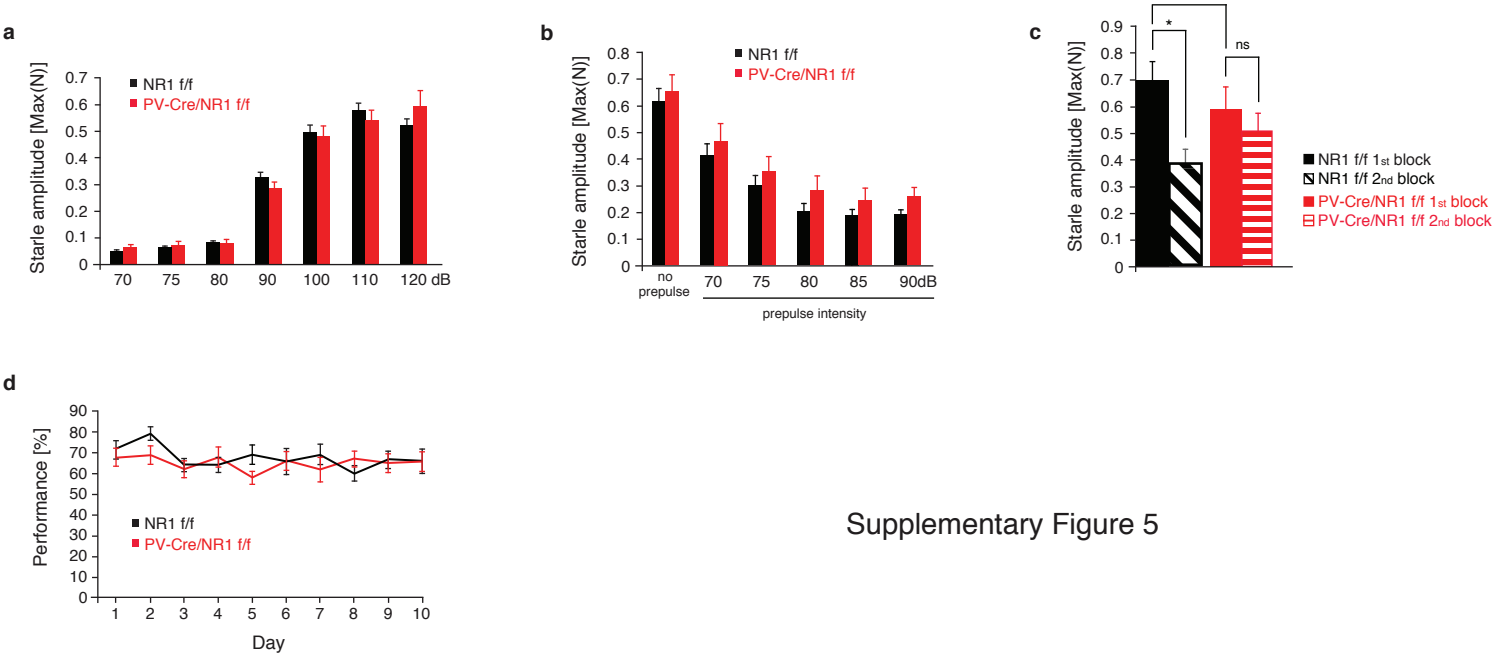

Supplementary Figure 5

SUPPLEMENTARY FIGURE LEGENDS

Supplementary Figure 1. Recombination in PV-Cre mice. At 8w near complete recombination can be seen in somatosensory cortex of PV-Cre mice. At 13 d, only scattered PV+ interneurons have recombined in somatosensory cortex (white arrowhead points to an example recombined cell). Scale bar: 200 μm.

Supplementary Figure 2. Impaired entrainment of spontaneous RS firing by FS-induced gamma oscillations in PV-Cre/NR1f/f mice. a, Population cycle histogram from 4 example RS cells in 3 PV-Cre/NR1f/f mice, showing a slightly elevated spontaneous firing rate, a smaller decrease in spike probability around 4-10 ms after the light flash, and a modest increase in spike probability around 20 ms. **b**, Population cycle histogram from 6 example FS cells recorded in the same experiments, showing a light-evoked peak in firing at 1-5 ms. **c**, Overlaid RS and FS population averages from the PV-Cre/NR1f/f mice. **d**, Population cycle histogram from 17 RS cells during gamma oscillation induction in 5 control PV-Cre mice, with 0 set as the time of the light flash on each cycle. The population average shows a decrease in spike probability around 4-10 ms after the light flash and an increase in spike probability around 20 ms. **e**, Population cycle histogram from 9 FS cells recorded in the same experiments, showing a light-evoked peak in firing at 1-2 ms. **f**, Overlaid RS and FS population averages from the PV-Cre control mice. **g**, Mean light-evoked spike latency for FS-PV+ interneurons in control mice was 2.62 ± 1.2 ms at low power (31 mW/mm2) and 1.18 ± 1.2 ms at high power (68 mW/mm2). Mean light-evoked spike latency for FS-PV+ interneurons in PV-Cre/NR1f/f

mice was significantly longer (4.52 ± 2.2 ms at low power and 2.74 ± 2.2 ms at high power; Mann-Whitney test; $P < 0.05$ in both cases). In addition, the variance of the spike latencies was significantly higher across cells in PV-Cre/NR1f/f mice than in control mice (F test; $P < 0.05$).

Supplementary Figure 3. Modeling on the role of NMDAR in FS-PV+ interneurons in the emergence of gamma rhythm. a, Frequency content for 30 cell computational model of baseline gamma power reduction in PV-Cre/NR1f/f mice (red) compared to control mice (black). Removal of NMDAR currents in the PV-Cre/NR1f/f network is modeled as a reduction in excitability of inhibitory cells (controlled using the model equivalent of applied current). Lighter region shows standard error over 5 trials. **b**, Using the same model and signal processing as in panel **a**, when excitability is reduced in excitatory as well as inhibitory cells, modeling an application of MK-801 (orange) to PV-Cre/NR1f/f mice, power in the gamma range is reduced. Lighter regions indicate standard error over 5 simulations. **c**, Model results showing increased latency and variation in FS cell response to optogenetic excitatory drive. Model contained a 10 cell inhibitory population, with some heterogeneity in baseline excitability (controlled using the model equivalent of applied current). Excitability is reduced to model PV-Cre/NR1f/f genetic alterations to fast spiking interneurons and results in increased latency and variance in time to spike after simulated optogenetic drive (200 ms of 40 Hz excitatory drive). Error bars show standard error across spikes. See Extended Materials and Methods in Supplementary Information for information on model construction and signal processing.

Supplementary Figure 4. Baseline cortical oscillations and NMDAR antagonist induced gamma rhythms in awake animals. a-d, LFP activity in somatosensory cortex in awake control (black) and PV-Cre/NR1f/f (red) mice. **a, b** Average relative power in the 6-10 Hz frequency band 15 min before administration of MK-801 (dashed line), to 35 min after. Lighter regions indicate s.e.m. **c**, **d** Average relative power in the 12-24 Hz frequency band 15 min before administration of MK-801 (dashed line), to 35 min after. Lighter regions indicate s.e.m. Pre, 5-15 min before MK-801; Post1, 5-15 min after MK-801; Post2, 25-35 min after MK-801. * $P < 0.05$; error bars, mean ± s.e.m.

Supplementary Figure 5. Acoustic startle response in PPI and habituation, and discrete paired-trial delayed alternation training in the T-maze. a, The startle response is normal in PV-Cre/NR1f/f mice. Startle response (Max(N)) from 70-120 dB in control (black) and PV-Cre/NR1f/f (red) mice. **b**, The mean startle amplitude (Max(N)) recorded during the PPI test in Figure 5a. There is no significant difference in response amplitude between the two genotypes at any prepulse intensity ($P > 0.05$ at all intensities). **c**, The mean startle amplitude (Max(N)) recorded during the habituation test in Figure 5b. The two genotypes display no significant difference in startle response to the first block of a 120 dB white noise stimulus. Control mice (NR1f/f; black) in contrast to PV-Cre/NR1f/f mice (red) show habituation by displaying significantly lower startle response to the second block of the 120 dB white noise stimulus. **d**, PV-Cre/NR1f/f and control mice learn the discrete paired-trial delayed alternation task similarly during the training at a 5 s retention interval. ns $P > 0.05$,*$P < 0.05$; error bars, mean ± s.e.m.